

A study of the impact properties of adhesively-bonded aluminum alloy based on impact velocity[†]

Teng Gao¹, Anthony J. Kinloch², Bamber R. K. Blackman², F. S. Rodriguez Sanchez², Sang-kyo Lee³, Chongdu Cho³, Hye-jin Bang⁴, Seong Sik Cheon⁵ and Jae Ung Cho^{5,*}

¹Department of Mechanical Engineering, Graduate School, Kongju National University, Cheonan, 331-717, Korea

²Department of Mechanical Engineering, Imperial College London, Exhibition Road, London SW7 2AZ, UK

³Department of Mechanical Engineering, Inha University, 402-751, Korea

⁴Department of Mechanical Engineering, Graduate School, Inha University, 402-751, Korea

⁵Division of Mechanical and Automotive Engineering, Kongju National University, Cheonan, 331-717, Korea

(Manuscript Received August 28, 2014; Revised October 11, 2014; Accepted October 17, 2014)

Abstract

In this study, an experiment and a simulation were carried out on colliding an adhesively-bonded tapered double cantilever beam (TDCB) at the impact velocities of 5 m/s, 7.5 m/s and 12.5 m/s. The analysis method of the corrected beam theory (CBT) was used to obtain the rate of energy release in the bonded area according to the crack progression, and a simulation was performed to determine the maximum strain energy during the impact analysis as a means to examine the mechanical properties of aluminium alloy. The experimental data were found to be higher than the simulation data. This is deemed to explicable by the fact that the adhesive strength was maintained even after the specimen separated in the experiment. Crack progression occurred, irrespective of the impact velocity, and high strain energy occurred at the end of the bonded region, thereby causing the strain energy to increase in the final stages. Also, the maximum load applied on the pin and the maximum strain energy in the bonded area were shown increase at higher impact velocities. The results of the experiment and simulation performed in this study are expected to serve as important data in developing a safety design for composite materials that can help prevent the progression of cracks caused by impact.

Keywords: Aluminium alloy; Crack; Energy release rate; Strain energy; Tapered double cantilever beam (TDCB)

1. Introduction

Carbon dioxide (CO₂) emissions contribute to global warming, and for this reason, there have been efforts to develop improved combustion, composite material and optimum design technologies as a means to reduce CO₂ emissions. In the recent years, there have been a growing number of firms manufacturing products using aluminium alloy, which can be used in the manufacture of aircraft, spacecraft, trains and production machines. Also, aluminium alloy, aluminium foam and plastic are used to make composite materials. A composite material is produced by combining and forming two or more types of material to exhibit properties that cannot be attained using a single material. In other words, it is a material produced through a macroscopic integration of two or more materials with different forms and/or constituents. Composite materials are drawing a great deal of attention and are applied widely as they are lighter than steel, but are characterized by

strong durability, excellent safety and high energy-saving effects. As for materials made using aluminium alloy, when they are fixed to a structure using bolts and nuts or the conventional welding method, it increases not only the processing time but also the weight and the aluminium alloy can become damaged and undergo deformation due to the pressure exerted by the bolts and nuts [1-5]. For this reason, there recently have been increasing uses of special adhesives such as an epoxy-based adhesive to attach aluminium alloy to a structure and due to the excellence of these adhesives, they are now being used for conventional metal materials [6-12]. Special adhesives, which can also be used to attach thin boards, produce low noise and vibration during their application. Although special adhesives present advantages compared to the conventional bonding technologies, there is a drawback that the adhesive strength in the bonded area can be lowered to a significant extent in the presence of an impact load [12-19]. In this study, a tapered double cantilever beam (TDCB) made of aluminium alloy was modelled and subjected to an impact load at the velocities of 5 m/s, 7.5 m/s, and 12.5 m/s. The experimental data were then analysed and the rate of energy

*Corresponding author. Tel.: +82 41 521 9271, Fax.: +82 41 555 9123

E-mail address: jucho@kongju.ac.kr

[†]Recommended by Chief-in-Editor Emeriti Haecheon Choi

© KSME & Springer 2015

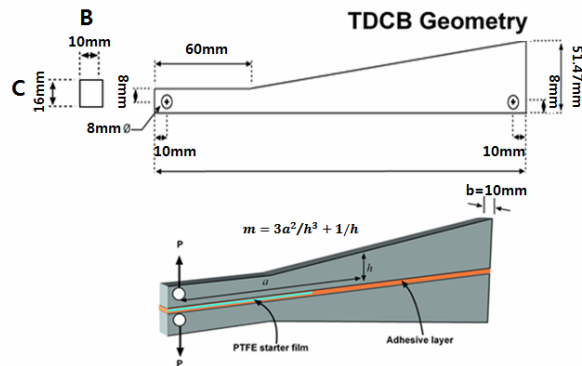


Fig. 1. Measurement of specimen.



Fig. 2. Experiment specimen.

release in the bonded area was determined based on CBT. ANSYS Design Modeller was used for a simulation, and a finite element analysis was conducted under the same conditions as the experiment. The results of the experiment and the simulation were compared in order to determine the mechanical properties of aluminium alloy in relation to impact. This study aims to enable the application of adhesively-bonded aluminium alloy in the composite materials used in car bumpers and aircraft fuel tanks and to identify the mechanical properties of the material and the effect of the impact load on the fracture energy. In addition, the findings of this study are expected to serve as important data in developing composite materials and their safety design [20-22].

2. Method of experiment and simulation

2.1 Experimental apparatus and model

The specimens used in the experiment were made using the aluminium alloy conforming to the British standard (BS 7991) and ISO standard (ISO 11343). The specimen dimensions are shown in Fig. 1. The incline of the model was represented as “*m*” and the distance between the centre of the pin hole and the end of the model was represented as “*a*”. Based on Eq. (1), when *m*=2 and *a*=300, the height (*h*) is 51.47 mm. The diameter of the pin hole was 8 mm, while the length and thickness of the TDCB model were 310 mm and 10 mm, respectively. The model fabricated based on Fig. 1 is shown in Fig. 2, which shows that the upper and lower parts of the

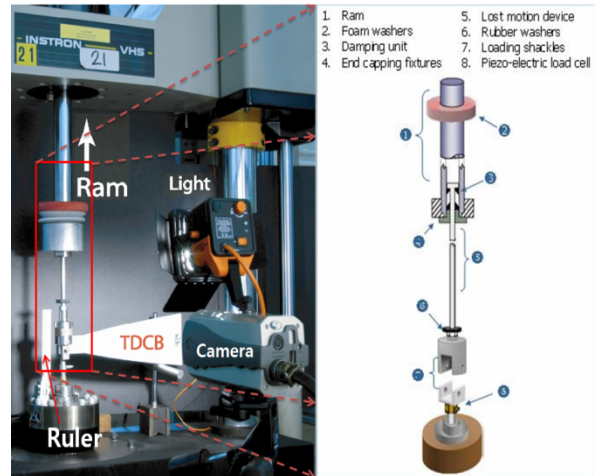


Fig. 3. Setup of aluminium alloy at impact tester.

model were attached using a red adhesive called XD4600. The specimen was oven cured at 180°C after the temperature was increased by 2°C over the course of 30 minutes. The thickness of the adhesion line was maintained at 0.4 mm using Ballotini (fine glass beads).

$$m = \frac{3a^2}{h^3} + \frac{1}{h} \tag{1}$$

In order to perform the impact experiment, the VHS 8800 high strain rate system, which can reach a maximum impact speed of 25 m/s, was used. The TDCB model was set in accordance with the impact equipment as shown in Fig. 3. The load block of the lower part of the TDCB was fixed, and the load block of the upper part was pulled.

The energy release rate can be determined based on the simple beam theory (SBT) or the corrected beam theory (CBT). SBT does not consider the actual shape of the beam, which has an incline, or the effect of the beam rotation, and the correction factor for the internal rotation at the end of the beam does not satisfy the American Society for Testing and Materials (ASTM) standards. Thus, CBT proposed by the European Structural Integrity Society was selected for this study.

2.2 Corrected beam theory (CBT)

The energy release rate, G_{IC} , under the load condition can be calculated using Eq. (2).

$$G_{IC} = \frac{P^2}{2B} \frac{dC}{da} \tag{2}$$

where *B* is the width of the specimen, *P* the load measured from the load cell of the testing equipment, and *a* the crack length. *C* is the compliance (δ / P) determined based on the bending and shearing strain. δ is the displacement due to *P*.

Table 1. Property of material.

Density (kg/m ³)	2720
Young's modulus (GPa)	72.4
Poisson's ratio	0.33
Ultimate tensile strength (MPa)	485
Yield tensile strength (MPa)	415

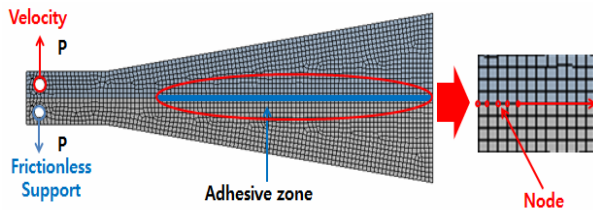


Fig. 4. Mesh of specimen.

Also, when the shape factor of the specimen m , is presumed to be irrespective of $1/h$, the correction for the shear force, dC/da can be calculated as follows:

$$\frac{dC}{da} = \frac{8m}{E_s B} \left[1 + 0.43 \left(\frac{3}{ma} \right)^{\frac{1}{3}} \right] \quad (3)$$

Thus, Eqs. (2) and (3) can be used to obtain Eq. (4), and the energy release rate, G_{IC} , under the load condition can be obtained.

$$G_{IC} = \frac{4P^2 m}{E_s B^2} \left[1 + 0.43 \left(\frac{3}{ma} \right)^{\frac{1}{3}} \right] \quad (4)$$

2.3 Simulation condition and model

A 2D model with the same shape as the specimen used in the experiment was created using the ANSYS design modeller. The meshes of 3D model are divided with the hexagonal elements. But the meshes of 2D model are divided with the tetragonal elements. As the thickness is applied into 2D model in analysis, the configuration can be embodied like 3D model. As the analysis time can be reduced. 2D model is more useful than 3D model in this study. Fig. 4 shows that the nodes were arranged in a straight line in the mesh, and this is very important in the expression of the adhesion simulation. Also, as shown in Fig. 4, there were 6,990 nodes and 2,172 elements in the TDCB model. The material of the model was Aluminium Alloy 2014, the properties of which are shown in Table 1.

The constraints set for the simulation were the same as those of the experiment. As shown in Fig. 4, the contact condition for the load block of the lower part of the TDCB model was frictionless support, and the velocity at which the load block of the upper part moved was set at 2.5 m/s, 7.5 m/s, and

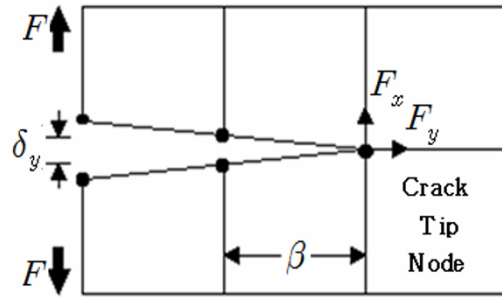


Fig. 5. Nodal force at crack tip.

12.5 m/s. At the frictionless support, the coefficient of friction is near 0 and the free sliding is allowed. The area where the upper and lower parts were bonded was to be 100 mm away from the load point to create a pre-cracked. The adhesion is to bond with adhesive between upper and lower parts of the specimen. Just before it falls apart, the bonding force becomes maximum. This bonding force is the strength of adhesive. As for adhesive strength between the upper and lower parts of the specimen, it was set at 8 MPa, which is the normal stress representing the maximum vertical force that can be withstood by the bonded part, and the gap between the upper and lower parts before the fracture was set at 0.6 mm. This state is virtually defined as the layer of adhesive. In the simulation, the method used to determine the energy release rate differed from the one used in the experiment. It is important to note that when the fracture energy exceeds the critical energy release rate (G_C) at the crack tip, the crack spreads. Because the simulation model was a 2D model, the energy release rate was obtained based on the load and displacement of the nodes at the crack tip as shown in Fig. 5, where β is the width of the crack tip and F_x , F_y , δ_x , and δ_y were the loads and displacements in the X and Y directions.

Thus, the critical energy release rate per unit thickness can be obtained using Eq. (5).

$$G_C = (F_x \delta_x + F_y \delta_y) / 2\beta \quad (5)$$

3. Results

3.1 Relation of load and displacement determined in the impact experiment and simulation at impact velocities of 5 m/s, 7.5 m/s and 12.5 m/s

Fig. 6 is a graph comparing the loads according to the load cell displacement at the impact velocities of 5 m/s, 7.5 m/s and 12.5 m/s. The black curve represents the data for the impact velocity of 5 m/s, the red curve the data for 7.5 m/s and the green curve the data for 12.5 m/s. The simulation data are indicated by circles, while the experimental data are indicated by squares. Generally, the maximum load was observed at a displacement of 5 to 7 mm, and the maximum load applied on the pin increased at higher impact velocities. In the experiment

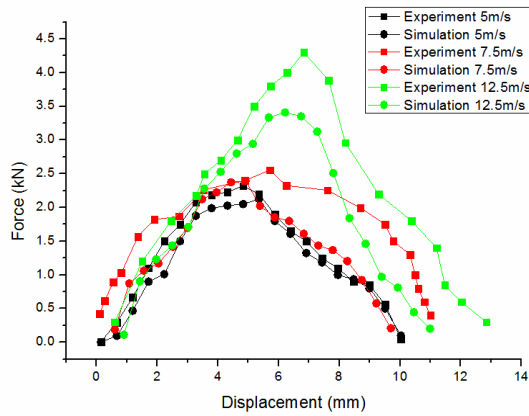


Fig. 6. Load according to displacement with experiment and simulation in cases of 5 m/s, 7.5 m/s and 12.5 m/s rates.

where the impact velocity was 5 m/s, a maximum load of 2.32 kN was observed at 4.83 mm, while a maximum load of 2.12 kN was observed at 5.35 mm in the simulation. As for impact velocity of 7.5 m/s, a maximum load of 2.55 kN was observed at 5.7 mm in the experiment, while a maximum load of 2.39 kN was observed at 4.91 mm in the simulation. As for impact velocity of 12.5 m/s, a maximum load of 4.3 kN was observed at 6.83 mm in the experiment, and a maximum load of 3.41 kN was observed at 6.21 mm in the simulation. As shown by Fig. 6, simulation result approaches experimental graph and has the similar trend as experiment.

3.2 Relation of energy release rate and crack length determined in the impact experiment and simulation at impact velocities of 5 m/s, 7.5 m/s and 12.5 m/s

Fig. 7 shows the energy release rate-crack length curves obtained through the experiment and simulation of the TDCB specimen made of aluminium alloy when impact was applied at a velocity of 5 m/s. The experimental values were generally higher than the simulation values, and this was because the adhesive strength was maintained even after the specimen separated in the experiment.

Because the load has a significant impact on the energy release rate, the rate increased at a similar slope in the experiment and simulation. In the experiment, the maximum energy release rate was observed to be 5,198.4 J/m², which differed from the simulation value by 440 J/m².

Fig. 2 is a graph of the energy release rate plotted against the crack length, and compares the results of the experiment and the simulation when the impact velocity was 7.5 m/s. The experimental and simulation values were similar, and the maximum energy release rates were nearly the same at about 6,800 J/m². As explained earlier, due to the significant impact of the load on the energy release rate, the maximum energy release rates determined in the experiment and simulation for the impact velocity of 7.5 m/s were higher than the maximum rates determined for 5 m/s.

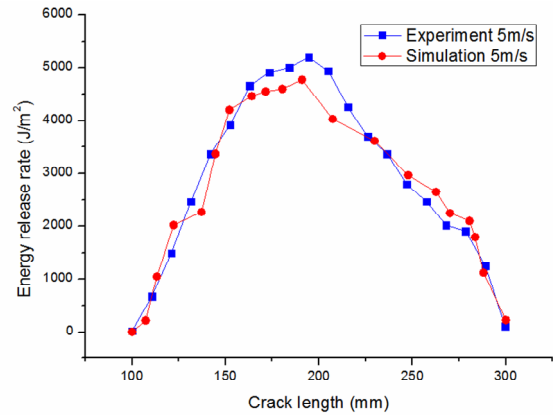


Fig. 7. Energy release rate according to crack length with experiment and simulation in case of 5 m/s rate.

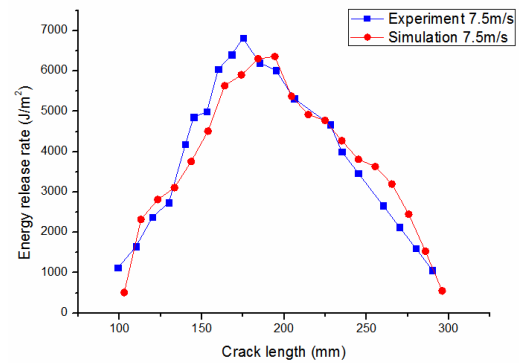


Fig. 8. Energy release rate according to crack length with experiment and simulation in case of 7.5 m/s rate.

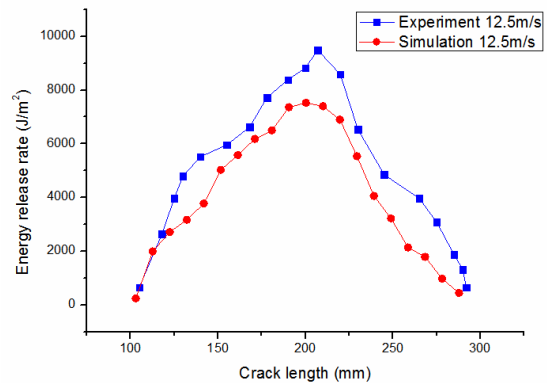


Fig. 9. Energy release rate according to crack length with experiment and simulation in case of 12.5 m/s rate.

Fig. 9 is a graph of the energy release rate occurring in the bonded area when the load block was applied on the specimen at an impact velocity of 12.5 m/s. The maximum energy release rate observed in the experiment was 9,400 J/m², which differed from the simulation value by 2,000 J/m². Figs. 7-9 show that the energy release rate in the bonded area increased at higher impact velocities. Combining these graphs is expected to produce a graph shown in Fig. 6 because the nodal

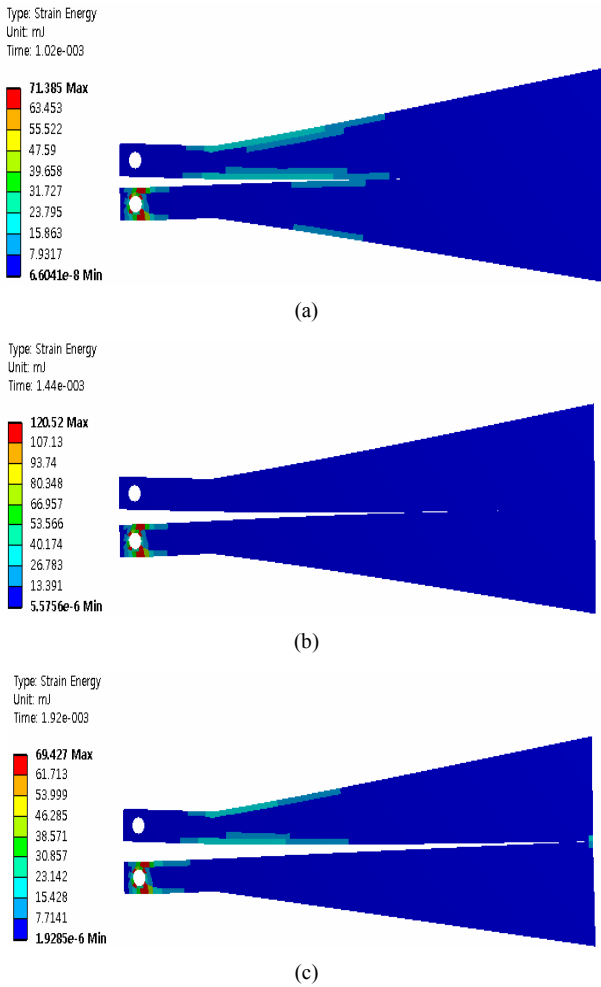


Fig. 10. (a) Contour of strain energy at impact analysis at 1.02 ms in case of impact velocity of 5 m/s; (b) contour of strain energy at impact analysis at 1.44 ms in case of impact velocity of 5 m/s; (c) contour of strain energy at impact analysis at 1.92 ms in case of impact velocities of 5 m/s.

load and displacement are expected to have a substantial impact on the energy release rate.

3.3 Strain energy at impact velocities of 5 m/s, 7.5 m/s and 12.5 m/s

Fig. 10 shows the strain energy occurring over time when the impact velocity was 5 m/s. The strain energy increase with increased load until it reached its maximum point at 1.44 ms. Also, Fig. 10(c) shows that the crack progressed from the end of the bonded area of the model, thereby resulting in high strain energy at the end. The results of the experiment when the impact velocities were 7.5 m/s and 12.5 m/s and the results of the simulation when the impact velocities were 5 m/s, 7.5 m/s and 12.5 m/s were similar.

Fig. 11 is a graph depicting the changes in the maximum strain energy over time for each of the impact velocities under

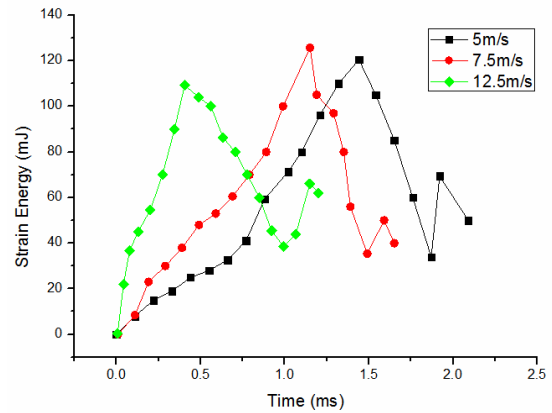


Fig. 11. Graph of strain energy due to time at impact analysis in cases of 5 m/s, 7.5 m/s and 12.5 m/s rates.

analysis. When the impact velocity was 5 m/s, the strain energy increase steadily before reaching its peak at 120.52 mJ and decrease rapidly as the bonded part became completely separated. As shown in Fig. 10, the strain energy at the end of the bonded area was high at time = 1.92 ms, and thus, the curve dropped to 34 mJ before increasing to 69 mJ at 1.92 ms. The curves for the impact velocities of 7.5 m/s and 12.5 m/s were similar in appearance as the curve for the impact velocity of 5 m/s. However, the strain energy when the impact velocity was 7.5 m/s and 12.5 m/s was 125.67 mJ and 109.26 mJ, respectively, and increased more sharply before dropping, compared to the curve for the impact velocity of 5 m/s. Also, the maximum strain energy for 12.5 m/s was smaller than the maximum values obtained for 5 m/s and 7.5 m/s. This was thought to be because when the impact velocity was 12.5 m/s, the specimen became damaged quickly and there was little stored energy in the area of deformation.

3.4 Equivalent stress at impact velocities of 5 m/s, 7.5 m/s and 12.5 m/s

Fig. 12 shows the equivalent curves of the equivalent stress at the time of maximum equivalent stress when the impact velocity was 5 m/s. When the equivalent stress attains the yield stress, the failure happens. The yield stress occurs at the layer of adhesive and the part of aluminum. Fig. 12(a) shows that an equivalent stress of 904 MPa occurred at the load cell in the lower part at 1.02 ms. It was determined that the load cell was damaged because the equivalent stress occurring at the load cell was bigger than the yield stress of the aluminium alloy. However, in the simulation, high equivalent stress occurred only on the surface of the load cell, and load cell was not broken as the equivalent stress was smaller than the yield stress in most areas. This was consistent with the shape observed in the experiment. Fig. 12(b) shows that a maximum equivalent stress of 1,173.9 MPa occurred in the load cell of the lower part at 1.44 ms, but in the simulation, the equivalent stress in other areas was shown to be maintained at around

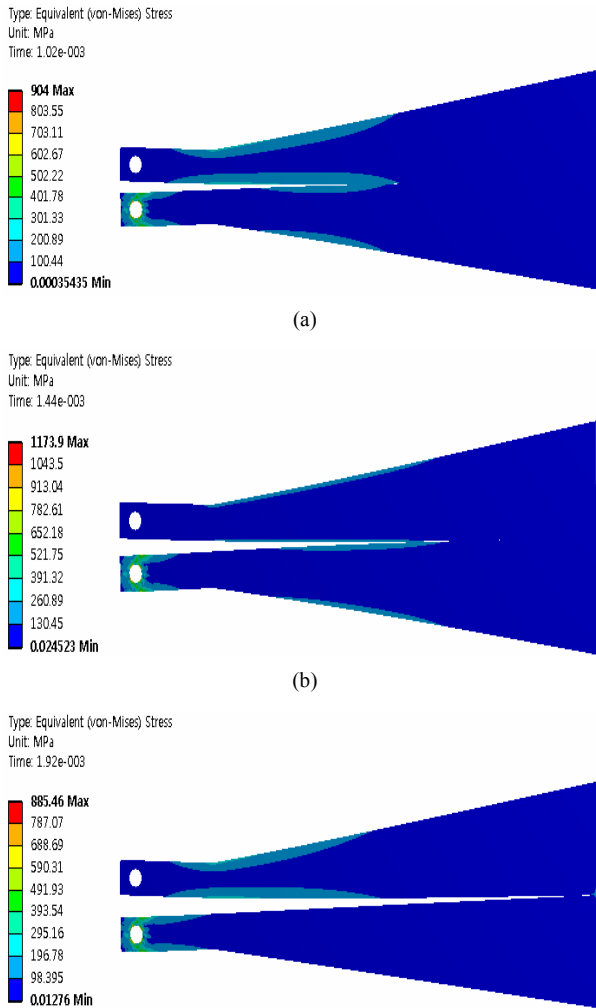


Fig. 12. (a) Contour of equivalent stress at impact analysis at 1.02 ms in case of impact velocity of 5 m/s; (b) contour of equivalent stress at impact analysis at 1.44 ms in case of impact velocity of 5 m/s; (c) contour of equivalent stress at impact analysis at 1.92 ms in case of impact velocity of 5 m/s.

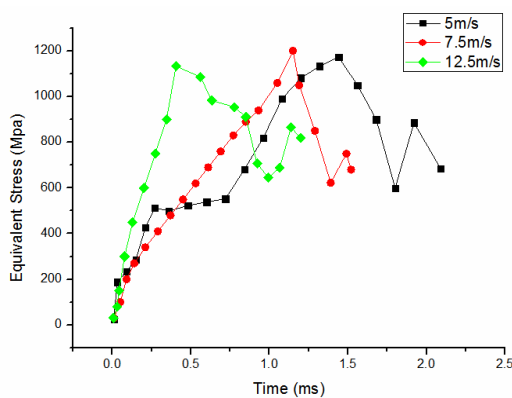


Fig. 13. Graph of equivalent stress due to time at impact analysis in cases of 5 m/s, 7.5 m/s and 12.5 m/s rates.

150 MPa. Fig. 12(c) shows that a maximum equivalent stress of 885.46 MPa occurred in the load cell of the lower part at 1.92 ms, and high equivalent stress occurred at the end of the bonded area.

Fig. 13 is a graph depicting the changes in the maximum equivalent stress over time based on the simulation results. The curve for the impact velocity of 5 m/s climbed steadily compared to the curves for 7.5 m/s and 12.5 m/s. As shown in Fig. 12(c), there was high equivalent stress at the end of the bonded area, and this caused the curves to drop down before climbing up again. Moreover, the maximum equivalent stress was determined to be 1200.7 MPa at an impact velocity of 7.5 m/s and 1133.6 MPa at an impact velocity of 12.5 m/s.

4. Conclusions

An impact experiment was conducted on a tapered double cantilever beam (TDCB) made of aluminium alloy at the impact velocities of 5 m/s, 7.5 m/s and 12.5 m/s and a simulation using a finite element model was performed for a numerical analysis. Based on the results of the experiment and the simulation, the following conclusions were reached:

- (1) The load generally increased as larger displacements before decreasing beyond a certain point. This was because the area of adhesion became smaller over time. Also, the maximum load applied on the pin increased at higher impact velocities.
- (2) The energy release rates determined in the experiment were mostly high. This was thought to be due to the fact that the adhesive strength was maintained even after the specimen became separated.
- (3) When the impact velocities were 5 m/s, 7.5 m/s and 12.5 m/s, the maximum strain energies were 120.52 mJ, 125.67 mJ and 109.26 mJ, and the maximum equivalent stresses of 1173.9 MPa, 1200.7 MPa and 1133.6 MPa, respectively. High equivalent stress was only observed on the surface of the load cell, and load cell was not broken as the equivalent stress was smaller than the yield stress in most areas.
- (4) Crack progression occurred, irrespective of the impact velocity, and high strain energy and equivalent stress occurred at the end of the bonded area, thereby causing the strain energy and equivalent stress to reach their peaks before falling and climbing back up again in repetition.
- (5) The simulation results obtained in this study are expected to serve as important data in developing composite materials and safety design thereof to prevent the progression of cracks caused by collision.

Acknowledgement

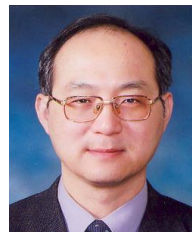
This research was supported by the Basic Science Research Program through the National Research Foundation of Korea (NRF) funded by the Ministry of Education, Science, and Technology (2011-0006548).

References

- [1] D. G. Lee, K. S. Kim and Y. T. Im, An experimental study of fatigue strength for adhesively bonded tubular single joints, *International Journal of Adhesives*, 35 (1991) 39-53.
- [2] C. Kadar, F. Chmelik and Z. Rajkovits, Acoustic emission measurements on metal foams [J], *Journal of Alloys and Compounds*, 378 (2003) 145-150.
- [3] J. Pang, Y. Du and K. Y. Wu, Fatigue analysis of adhesive joints under vibration loading, *International Journal of Adhesion & Adhesives*, 89 (2013) 899-920.
- [4] R. C. Batra and Z. Peng, Development of shear bands in dynamic plane strain compression of depleted uranium and tungsten blocks [J], *International Journal of Impact Engineering*, 16 (3) (1995) 375-395.
- [5] L. D. Kenny, Mechanical properties of particle stabilized aluminum foam [J], *Materials Science Forum*, 217-222 (3) (1996) 1883-1890.
- [6] P. Briskham and G. Smith, Cyclic stress durability testing of lap shear joints exposed to hot-wet conditions, *International Journal of Adhesion and Adhesives*, 20 (1) (2000) 33-38.
- [7] T. Mukai, T. Miyoshi, S. Nakano, H. Somekawa and K. Higashi, Compressive response of a closed-cell aluminum foam at high strain rate [J], *Scripta Materialia*, 54 (4) (2006) 533-537.
- [8] J. U. Cho, S. J. Hong, S. K. Lee and C. Cho, Impact fracture behavior at the material of aluminum foam [J], *Materials Science and Engineering A*, 539 (2012) 250-258.
- [9] X. Teng and T. Wierzbicki, Dynamic shear plugging of beams and plates with an advancing crack [J], *International Journal of Impact Engineering*, 31 (2005) 667-698.
- [10] T. Børvik, O. S. Hopperstad, M. Langseth and K. A. Malo, Effects of target thickness in blunt projectile penetration of Weldox 460 E steel plates [J], *International Journal of Impact Engineering*, 28 (4) (2003) 413-464.
- [11] X. W. Chen and Q. M. Li, Shear plugging and perforation of ductile circular plates struck by a blunt projectile [J], *International Journal of Impact Engineering*, 28 (2003) 513-536.
- [12] A. Pirondi and G. Nicoletto, Fatigue crack growth in bonded DCB specimens, *Engineering Fracture Mechanics*, 71 (2004) 859-871.
- [13] M. M. Shokrieh, M. Heidari-Rarani and S. Rahimi, Influence of curved delamination front on toughness of multidirectional DCB specimens, *Composite Structures*, 94 (4) (2012) 1359-1365.
- [14] B. R. K. Blackman, J. P. Dear, A. J. Kinloch, H. MacGillivray, Y. Wang, J. G. Williams and P. Yayla, The failure of fibre composites and adhesively bonded fibre composites under high rates of test part III mixed-mode I/II and mode II loadings, *Journal of Materials Science*, 31 (17) 4467-4477.
- [15] K. R. Pradeep, B. Nageswara Rao, S. M. Srinivasan and K. Balasubramaniam, Interface fracture assessment on honeycomb sandwich composite DCB specimens, *Engineering Fracture Mechanics*, 93 (2012) 108-118.
- [16] S. Marzi, A. Biel and U. Stigh, On experimental methods to investigate the effect of layer thickness on the fracture behavior of adhesively bonded joints, *International Journal of Adhesion and Adhesives*, 31 (8) (2011) 840-850.
- [17] P. Qiao, J. Wang and J. F. Davalos, Tapered beam on elastic foundation model for compliance rate change of TDCB Specimen, *Engineering Fracture Mechanics*, 70 (2) (2003) 339-353.
- [18] J. U. Cho, A. Kinloch, B. Blackman, S. Rodriguez, C. D. Cho and S. K. Lee, Fracture behavior of adhesively-bonded composite materials under impact loading, *International Journal of Precision Engineering and Manufacturing*, 11 (1) (2010) 89-95.
- [19] V. Cooper, A. Ivankovic, A. Karac, D. McAuliffe and N. Murphy, Effects of bond gap thickness on the fracture of nano-toughened epoxy adhesive joints, *Polymer*, 53 (24) (2012) 5540-5553.
- [20] N. Michailidis, F. Stergioudi, H. Omar and D. N. Tsipas, An image-based reconstruction of the 3D geometry of an Al open-cell foam and FEM modeling of the material response, *Mechanics of Materials*, 42 (2) (2010) 142-147.
- [21] S. K. Parida and A. K. Pradhan, 3D finite element analysis of stress distributions and strain energy release rates for adhesive bonded flat composite lap shear joints having pre-existing delaminations, *Journal of Mechanical Science and Technology*, 28 (2) (2014) 481-488.
- [22] J. U. Cho, S. K. Lee, C. Cho, F. S. Rodriguez Sanchez, B. R. K. Blackman and A. J. Kinloch, A study on the impact behavior of adhesively-bonded composite materials, *Journal of Mechanical Science and Technology*, 21 (10) (2007) 1671-1676.



Teng-Gao received his B.S. degree in Div. of Mechanical & Automotive Engineering from Kongju University, Korea, in 2013. Now he is at the course of M.S. degree in Mechanical Engineering at Graduate School of Kongju University. He is interested in the areas of fracture mechanics (dynamic impact), composite material, fatigue and strength evaluation.



Jae-Ung Cho received his M.S. and Doctor Degrees in Mechanical Engineering from Inha University, Incheon, Korea, in 1982 and 1986, respectively. Now he is a professor in Mechanical & Automotive Engineering of Kongju National University, Korea. He is interested in the areas of fracture mechanics (dynamic impact), composite material, fatigue and strength evaluation, and so on.